JOURNAL OF CATALYSIS **170,** 402–410 (1997)
ARTICLE NO. CA971753

RuS_2(111) Surfaces: Theoretical Study of Various Terminations and Their Interaction with H_2

F. Frechard[1] and P. Sautet

Institut de Recherches sur la Catalyse, CNRS, 2 Avenue Einstein, 69626 Villeurbanne Cedex, France; and Laboratoire de Chimie Théorique, Ecole Normale Supérieure, 46 Allée d'Italie, 69364 Lyon Cedex 07, France

Received April 3, 1997; revised May 14, 1997; accepted May 14, 1997

Several surface terminations for RuS_2(111) have been compared on the basis of theoretical calculations. Hartree–Fock Periodic calculations with a posteriori evaluation of the correlation energy with a density functional approach have been used. The surfaces with an excess of S atoms compared to the RuS_2 stoichiometry are found to be more stable, the most stable one having seven S atoms at the surface for the unit cell. Depending on the amount of surface S, the S binding energy varies in a large interval and is smaller for atoms in a S_2 pair than for isolated S atoms. Dissociation of H_2 is strongly exothermic on these surfaces, giving generally SH groups but also Ru–H bonds for highly reduced surfaces. These calculations enable the building of a model and an energy profile for the reduction process of the RuS_2 surface. © 1997 Academic Press

I. INTRODUCTION

Sulfur removal from petroleum derivatives is a very important industrial process. The interest for efficient catalyst materials for hydrodesulfurization reactions has been strengthened recently by more drastic regulations in order to limit sulfur compounds in car exhausts. While the standard catalyst is a sulfide of molybdenum doped with Ni or Co, recent interest has appeared in the academic area for the sulfide of Ru, RuS_2. Over many other single metal sulfides (including MoS_2), RuS_2 has been shown to be the most active for the hydrodesulfurization of thiophene (1, 2).

Moreover, this sulfide material presents an important structural singularity: all S atoms are bonded in S_2 units. The structure can indeed be viewed as S_2 molecules distributed on the edges and center of a face centered cubic array of Ru atoms, the S–S bond being elongated to 2.17 Å compared to the gas phase value (1.89 Å). This situation contrasts with the case of MoS_2, which has been the subject of several experimental and theoretical studies (3–10), and that shows isolated S atoms in the crystal structure. It seems clear that such a structural singularity must induce specific behaviors for RuS_2 surface, chemisorption, and reaction properties. This, in our opinion, motivated a theoretical study of such properties for RuS_2, since it was not possible to directly extend the partial knowledge obtained for MoS_2, due to the markedly different environment of S atoms in the structure.

Our study was initiated by a recent experimental study of RuS_2 catalysts by Lacroix and co-workers (11–13). The reactivity for H_2–D_2 exchange was simultaneously correlated with the extent of prereduction of the catalyst and with the apparition, in H^1-NMR or inelastic neutron scattering spectra, of hydride Ru–H hydrogen species instead of proton-like S–H entities for the less reactive and less reduced samples.

In a previous paper (14), the chemisorption of H_2 and H_2S on a (100) surface of RuS_2 has been presented. This surface was shown to be rather unreactive, with a molecular chemisorption for H_2 and H_2S as the most stable situation. This can be associated with the fact that the (100) surface is a stable surface that results from preferential cleavage of the 3D structure of RuS_2. Moreover the S–S pairs in the solid are not broken at this (100) surface. As is well known in the case of MoS_2, the most stable surface plane is often not the most catalytically active one and the chemical reaction can take place at a minority more unsaturated centers (the slab edges for MoS_2). We present here the results of theoretical investigations of the structure, electronic structure, and H_2 chemisorption for the (111) face of RuS_2 which has been shown to appear with (100) faces on single crystal RuS_2 particles (15, 16).

If the stable termination of the (100) surface is rather clear, this is not the case for the (111) surface. Therefore, nine possible terminations have been considered, with different numbers of S layers at the surface, that depict various S stoichiometries from S-enriched to S-deficient situations. The electronic structure of the bare stoichiometric (111) surface was already described in a previous paper (17). In Section II the calculation methods will be briefly recalled. The various surface terminations will be compared and the electronic structure of three selected surface terminations

[1] Present address: Laboratory of Inorganic Chemistry and Catalysis, Eindhoven University of Technology, P.O. Box 513, 5600 MB Eindhoven, The Netherlands.

0021-9517/97 $25.00
Copyright © 1997 by Academic Press
All rights of reproduction in any form reserved.

will be detailed in Section III. The chemisorption of H_2 on the three selected surfaces will be considered in Section IV, and a model of surface reduction process will be proposed in Section V.

II. METHOD OF CALCULATION AND MODEL FOR THE (111) SURFACE

The CRYSTAL95 program (18) has been used to perform periodic Hartree–Fock (HF) calculations. The details and implementation of this method have been published elsewhere (19). CRYSTAL95 allows one to solve self-consistently the HF equations for a periodic system and therefore study crystals and surfaces without having to model them by a cluster, which is a frequently used approximation. The Hartree–Fock energy is corrected by a density functional (20) type calculation (21, 22). This inclusion of the influence of the electronic correlation tends in our case to increase the binding energy between atoms compared to the HF solution. For the RuS_2 bulk the optimum geometry corresponds to a cell parameter **a** of 5.55 Å (1% shorter than the 5.61 Å experimental value) and a crystallographic coordinate **u** of 0.393 (0.388 experimentally). The resulting bond lengths are 2.06 Å for S–S bond (2.17 Å experimental) and 2.34 Å for the Ru–S bond (2.35 Å experimental), the various angles being in very good agreement with experiment. As one could expect, the DFT correlation corrections do not change qualitatively the HF results but allow the introduction of a more quantitative approach for the relative energies. The local atomic orbital basis functions are developed, as usual, on a linear combination of Gaussian-type orbitals (GTO) and core electrons have been modeled by well-assessed effective-core-potential (ECP) techniques (23, 24). Split-valence functions have been used for all atoms (14). A good accuracy is used in the calculation for the cutoff of the integrals and the sampling in the *k*-space has been performed within a set of eight Monkhorst *k*-points in the irreducible Brillouin zone.

The surface is described by a slab, periodic in the *x* and *y* directions and finite in the orthogonal *z* direction. The arrangement of the (111) planes is composed of four planes of S between two planes of Ru. The S_2 pairs do not cross the Ru planes like for the (100) planes and two types are present: perpendicular ([111] direction) or tilted ([11-1] directions, etc.) relative to the (111) planes. The S atoms in the perpendicular pairs (Sp) are bonded to the Ru atoms from the closest plane, while the S atoms from the tilted pairs (St) are bonded to only two Ru atoms from the closest plane, the third bond being with a Ru atom from the other plane. Figure 1 depicts a slab made of 14 layers—4 central S layers between 2 Ru layers surrounded by 4 S layers on each side. The minimal cell needed to describe this slab is hexagonal, and its symmetry elements are an inversion center, three C_3 axes, and the related S_6 axes. These symmetry operations are used by the program and they have been kept for the entire study, even if this requirement to keep the symmetries reduces the choice for the surface modifications or for the adsorption sites (breaking these symmetries would make the calculations impossible). The C_3 axes are located on the Sp but also on some Ru atoms. It is possible to distinguish the different species of S atoms present on the surface (see Fig. 1). The more external S_1 is from the perpendicular pair and compared to the bulk situation it has its three Ru–S bonds missing, only linked to the other Sp (S_4) which is bonded to three Ru atoms. Between these 2 layers there are the six S atoms from the three tilted pairs in the unit cell; the more external S_2 are bonded to only one Ru atom (two Ru–S bonds missing), the other S atoms (S_3) being linked to two Ru atoms (one Ru–S bond missing). There are two inequivalent Ru species: the first one Ru_1 is unique in the cell and is located on a C_3 axis and the second type Ru_2 has three representatives in the cell that are related by a C_3 axis. For the inner S atoms only two species are present depending if the S atom is within the perpendicular pair (S_5) or in the three tilted pairs (S_6). The adsorbates will be symmetrically chemisorbed on both sides of the slab.

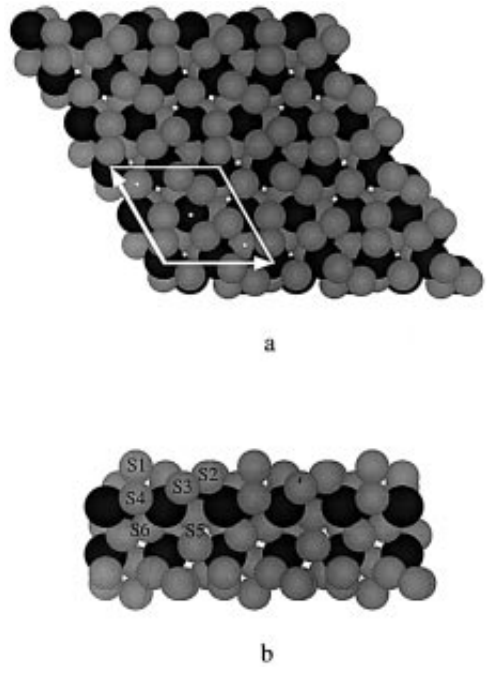

FIG. 1. A ball representation of a S-saturated bulk-termination $RuS_2(111)$ surface. (a) Top view; (b) side view that displays the possible arrangement of S_2 pairs (perpendicular and tilted), the C_3 axes (white dots on (a)), the surface unit cell, and the various inequivalent S and Ru atoms (Ru atoms are black and S atoms are gray).

Forces calculations are not possible with CRYSTAL, so a partial manual geometry optimization has been undertaken in order to determine, with the symmetry constraints, the relaxed geometries for the bare surface and with the adsorbates. The two Ru and the four inner S layers are kept

frozen and will refer to the optimized geometry found for the bulk (details for geometry optimizations are given in the corresponding sections).

III. POSSIBLE TERMINATIONS OF THE BARE SURFACE

Starting from the S-saturated (111) surface presented above and by removing first the external S atom from a pair, it is possible to construct eight other surface terminations, keeping the threefold axis symmetries. The nine terminations are shown in Fig. 2 and are labeled as a function of the number of S atoms present above the Ru plane on one side of the cell (per surface unit cell). For the S-saturated surfaces (model 8), three tilted pairs (only one is represented) and one perpendicular pair are located on one side of the cell. It is not possible to directly compare the total energies of those slabs since they do not contain the same number of S atoms. In order to compare their stabilities, we considered that the removed S atoms are combined in S_2 molecules in the gas phase (S_6 and S_8 cyclic molecules are more stable by around 10 kcal · mol^{-1} of S atom, but this does not change the tendencies). For each surface termination, the vertical positions of the S atoms have been optimized. In the case of surface 4, optimization of the horizontal positions of the three bridged S atoms remaining from the tilted pairs gave an energy gain inferior to 5 kcal · mol^{-1} in the surface unit cell. Except surface 8, for which the geometry has be taken from surfaces 7 and 5, all the surface geometries have been individually optimized with a step of 0.05 Å for the vertical positions of the S atoms, which is sufficient for a precision of around 2 kcal · mol^{-1} for the surface cell.

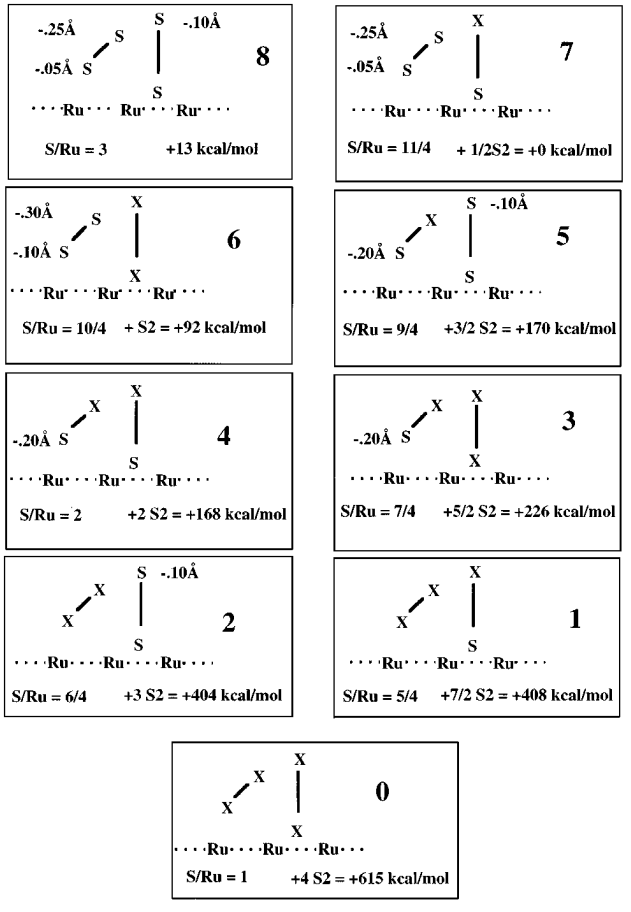

FIG. 2. Schematic of the various terminations considered for the RuS_2(111) surface. For each surface unit cell, three tilted S_2 pairs (only one shown) and one perpendicular S_2 pair can be at the surface. Each removed S atom is replaced by an X and the number of S atoms at the surface per unit cell corresponds to the label of the model. The surface stoichiometry, the number of S_2 molecules formed compared to model 8 and the total energy are given. The most stable model 7 is used as a reference for the energy. The vertical relaxation (Å) of the surface S layers are indicated, when these relaxations are significant.

The surfaces with a large concentration of S atoms are found to be generally more stable and the most stable situation is obtained for surface 7. This is in agreement with the excess S atoms in the experimental stoichiometry before reduction. The S–S bond within the perpendicular pair is weaker than for gas phase S_2 molecule (−13 kcal · mol^{-1} for model 8, −2 kcal · mol^{-1} for model 5), except for the highly unsaturated and unstable surface 2. Perpendicular pairs are therefore not stable at the surface. Breaking the tilted pairs (and making an equivalent number of 1/2 S_2 molecules) is on the contrary endothermic by 52, 56, and 44 kcal · mol^{-1} for the models 8, 7, and 6, respectively. Removing an isolated S atom is even more difficult, the transformation into S_2 molecules being endothermic by 92, 78, 58, 80, 130, and 207 kcal · mol^{-1} for models 7, 5, 4 (threefold S), 4 (twofold S), 3, and 1, respectively. The atomic binding energies of S atoms at the surface can be deduced from all the previous values by adding half of the calculated S_2 formation energy, i.e., 37 kcal · mol^{-1}. Therefore, there are three types of S atoms at the surface: weakly bound (or unstable) S from perpendicular S_2 pairs, intermediate bond for S from tilted pairs, and strongly bound atomic S. Such a range of S binding energies is specific to this RuS_2 surface, which depending on the S concentration shows different types of surface species. From this order of binding energies, it can also be deduced that it is not favorable to have at the same time a full pair and a missing adatom on the surface. The only realistic terminations are hence models 7, 4, 3, 1, and 0. Model 6, for example, is not stable and would transform in a domain of model 7 and a domain of model 4. The models where the surface is highly depleted in S atoms are strongly susceptible to undergoing reconstructions in order to stabilize the surface, such as bonds between Ru atoms, that could not be considered in this approach. This explains the high S binding energy for model 1, and these highly reduced models should be considered with caution.

The vertical relaxation of the S layers, relative to their position in the bulk, is also indicated in Fig. 2, except for the lowest layer of threefold S atoms where this relaxation

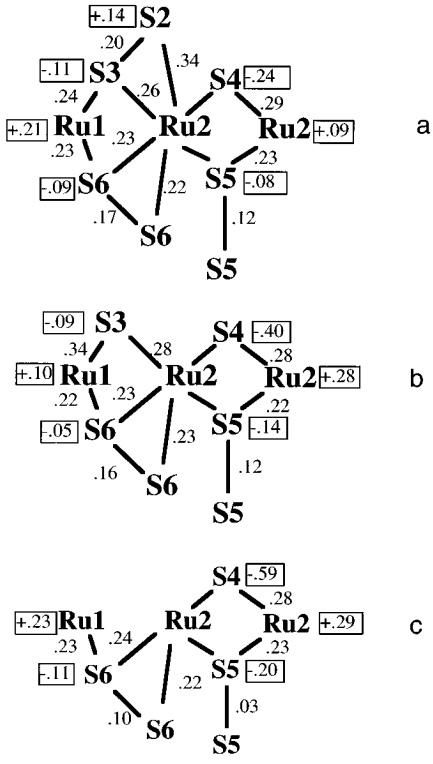

FIG. 3. Atomic charges (in a box) and overlap populations for model 7 (a), model 4 (b), and model 1 (c) of the surface.

is small. All S layers show an inward relaxation as it could be expected from the loss of bonding at the interface compared to the bulk situation, which tends to be compensated by a stronger interaction with the surface Ru atoms. The top-most atom of a vertical S–S pair shows a −0.1 Å displacement in the (unstable) situations where this atom is present. Otherwise, the relaxation is more important in the tilted pair (up to −0.3 Å displacement) and mostly affects the S atoms at the surface.

We will focus on the representative surfaces 7 (overstoichiometric with S/Ru = 11/4), 4 (stoichiometric with S/Ru = 2), and 1 (substoichiometric with S/Ru = 5/4). These surfaces will also be used for the hydrogen adsorption in the next section. The behavior of those three surfaces will be analyzed with the Mülliken electronic populations of the atoms (net charges and overlap populations) and also their related electronic structures will be detailed with the projected densities of states (PDOS). In order to get a reference we recall the net charges obtained for the optimized bulk with the same basis set and which are +0.16 for Ru and −0.08 for S while the overlap populations are +0.16 and +0.24 for S–S and Ru–S bonds, respectively. For clarity the atoms will be numbered as shown in Fig. 1, S_2 and S_3 belonging to an inclined pair, S_1 and S_4 to the perpendicular one, while Ru_1 is located on a C_3 axis and Ru_2 are the remaining atoms.

Surface 7 is similar to the previous one depicted in Fig. 1b, except that S_1 is removed, and the electronic populations are displayed in Fig. 3a. The S_2 atom is slightly positive: as a consequence of the two Ru–S_2 bonds cleaved at the surface, the p_x and p_y levels of this atom are mainly involved in weak π interactions with the Ru_2 atom. These orbitals contribute to antibonding contributions above the Fermi level forming the surface state seen in Fig. 4a. On the contrary, the S_4 atom has its p_x and p_y levels stabilized by the three bonds and its p_z lone pair pointing away from the surface appears as a narrow peak below the Fermi level (−9 eV). This atom then holds a significant negative charge of −0.24 e. The low-lying unoccupied surface state located on S_2 and the lone pair of S_4 should interact preferentially with the adsorbates

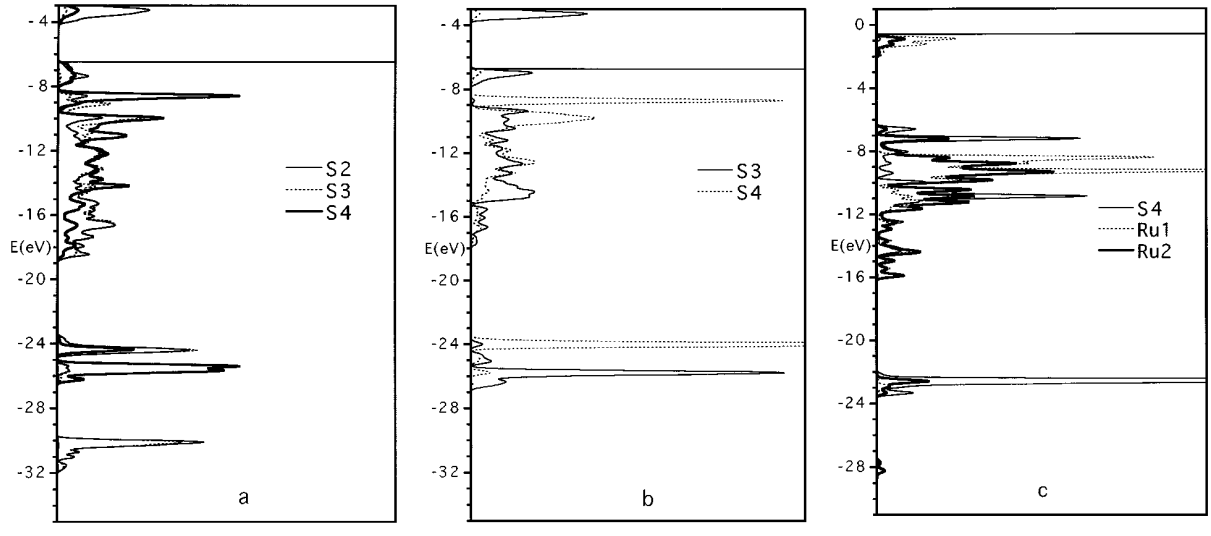

FIG. 4. Projected density of states on the surface atoms: (a) on the S_2, S_3, S_4 atoms of model 7; (b) on the S_3 and S_4 atoms of model 4; (c) on the S_4, Ru_1, Ru_2 atoms of model 1.

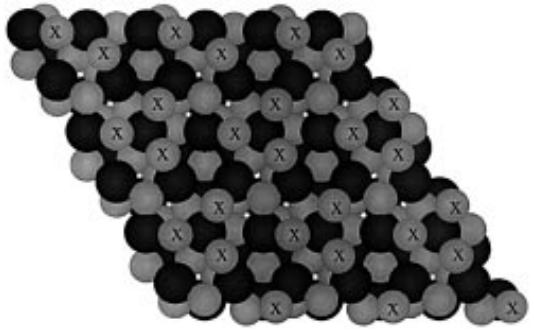

FIG. 5. A top view representation of the model 4 of the surface (Ru atoms are black and S atoms are gray). Model 1 can be obtained by removing the bridge S_3 atoms (labeled by X).

as they can be qualitatively identified as the "HOMO" and "LUMO" of the surface. For the overlap population values, the main difference with the bulk is a strengthening of the S–Ru bonds at the surface, especially S_2–Ru_2, and this is an illustration of the bond order conservation principle (25) with a partial compensation of unsaturations created at the surface. This is in clear relation with the inward relaxation of this surface S layer in model 7.

By removing the three S_2 atoms from surface 7, one obtains the stoichiometric surface 4 (Fig. 5) which does not have any more surface S–S pairs but the threefold S_4 and three bridged S_3 atoms (labeled by X in Fig. 5), while a vacancy appears on the Ru_2 atoms. This surface has been studied in Ref. (17) and we will only recall its main characteristics. The occupied and vacant surface states are now localized on the S_3 atom, as a combination of the p_x and p_y orbitals. This forms, below the Fermi level, a *p*-like lone pair parallel to the surface and perpendicular to the Ru_1–S_3–Ru_2 plane and, above the Fermi level, an antibonding state with an important contribution from the Ru atoms (Fig. 4b). The net charge on S_3 is slightly negative (Fig. 3b) but significantly less than that on S_4 which mainly presents a high-lying lone pair in the PDOS. S_3 (and to a smaller extent S_4) are then reactive sites at the surface. In order to decrease the unsaturation of the bridge S_3 atom (X), an *x*–*y* optimization was also performed for this atom. However, the displacement of S_3 toward a threefold site is found to be unfavorable for the energy. The Ru_1–S_3 and Ru_2–S_3 bonds were found to be slightly unequivalent, but this does not change the structure of the surface states.

Eliminating the bridged S_3 atoms (X in Fig. 5) gives the sulfur poor surface model 1 with only the S_4 atom remaining. Now the Ru_1 and Ru_2 atoms are easily accessible with three and two vacancies, respectively. In order to compensate these unsaturations, the Ru atoms interact strongly with the inner S–S pairs. The main effect is the lowering under the Fermi level and filling of some antibonding levels of the S–S pairs, which results in a weakening of the S–S bonds (Fig. 3c, this is particularly apparent for the S_5–S_5 pair). The new feature appearing in Fig. 4c is the high energy occupied surface states, which are now mainly localized on the Ru atoms. The peaks on the S_4 atom remain in the same energy range as before, with a significant negative charge on the atom. This high-lying surface state gives to the surface a reactive and unstable character.

IV. CHEMISORPTION OF H_2 ON THE RuS_2(111) SURFACES

The chemisorption of H_2 has been studied on the three selected models, corresponding to sulfur-rich (model 7), stoichiometric (model 4), and sulfur-poor (model 1) surfaces. In contrast with the (100) surface, a dissociated structure is favored for all considered terminations, and the energies for the dissociation cases are markedly lower than the metastable molecular configurations. The optimization procedure is identical to the bare surfaces for the surface S atoms but the angular positions of the hydrogen atoms were also optimized (by steps of 5°) while the S–H distance was fixed to 1.35 Å (a reasonable value regarding our previous study (14)). For the Ru–H bonds the distance and angles were optimized.

The best chemisorption situation for the sulfur-rich surface 7 is shown in Fig. 6. Two H_2 molecules can be dissociated per surface unit cell, and each terminal S atom is linked to a H atom, giving a –S–H unit (vertical by symmetry constraints) and three tilted –S–S–H fragments with

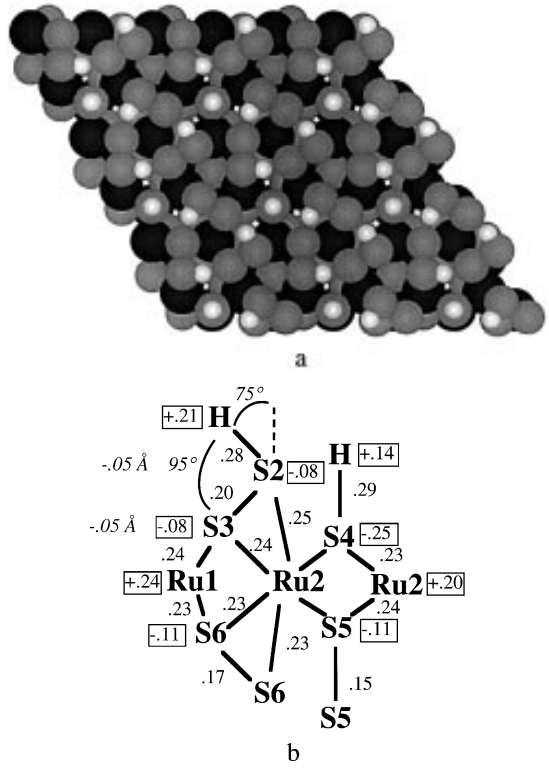

FIG. 6. A top view representation of the hydrogenated model 7 of the surface (Ru atoms are black, S atoms are gray, and H atoms are white) and a schematic describing some structural elements, the atomic charges (in a box) and overlap populations (*z* values for S_3 and S_2 refer to the bulk).

an optimized angle of 95° for (S,S,H) and a 75° tilt between H–S_2–S_3 and the vertical S_3–S_2–Ru_2 planes. The S_2–H bonds therefore have a strong inclination on the surface as it can be clearly seen on the top view. Indeed, H interacts with the surface states which are mainly localized on S3*p* orbitals parallel to the surface, and a second minimum has been found with the tilt in the other direction, only 16 kcal · mol^{-1} less stable. From Fig. 6b, both types of H atoms have a partial positive charge (and then have as expected a proton-like character) while the S–Ru bond overlap populations are significantly weakened by the H chemisorption (compare with Fig. 3a). In contrast, the S–S bond is not greatly affected by the chemisorption, bonding, and antibonding S–S contributions modified in a similar way. In this most stable chemisorption situation the binding energy, normalized to one H_2 molecule, is −100 kcal · mol^{-1}. The strong interaction is related with the presence of surface states on surface 7 that are mainly centered on S_2 and S_4. The H adsorption saturates the surface dangling bonds and the surface states disappear (Fig. 7a). While it can be suspected

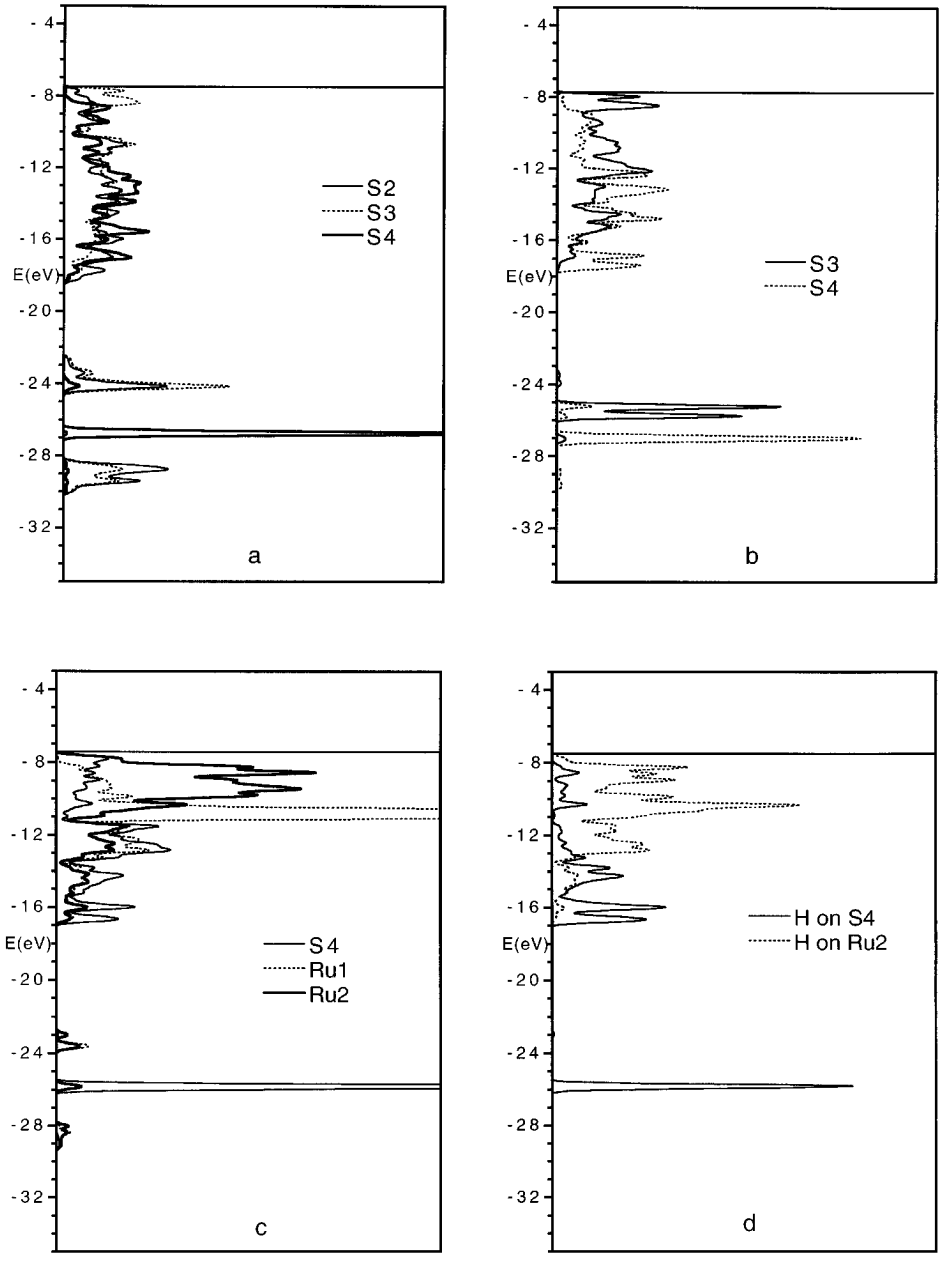

FIG. 7. Projected density of states on the surface atoms: (a) on the S_2, S_3, S_4 atoms of hydrogenated model 7; (b) on the S_3 and S_4 atoms of the hydrogenated model 4; (c) on the S_4, Ru_1, and Ru_2 atoms of the hydrogenated model 1; (d) on the H atoms for the hydrogenated model 1 (with a magnified scale). Curves for the proton-like and the hydride-like H atoms have a clearly different shape.

that surface 7 could undergo a reconstruction to stabilize its electronic structure, which could not be achieved by the partial optimization performed here, the hydrogenated surface seems on the contrary really stable. The situation can be compared to the well-known case of the Si(111) surface, where the bare surface shows various types of complicated reconstructions, while the H-terminated structure is very stable and has a simple (1×1) structure. Another energy minimum was found with the H atom bound to S_3 instead of S_2 on the S–S pair; however, it is 23 kcal · mol^{-1} less stable than the previous one.

For the stoichiometric model of surface 4, both S–S units at the surface are broken, and all hydrogen atoms interact with an "isolated" S atom (Fig. 8). Therefore, the situation is more even, and the surface S–H bonds are similar with a small positive charge on the H atoms. Despite the apparent accessibility of the Ru atoms, they are still well saturated by the S atoms, and an attempted adsorption of H on the metal atom resulted in a less favorable energy. The H–S_3 bond is situated in a vertical plane perpendicular to the Ru_1–S_3–Ru_2 plane with an angle of 45° with the vertical. The adsorption energy is −113 kcal · mol^{-1} (normalized to one H_2 molecule), significantly larger than that of surface 7 due to the stronger unsaturation and the marked surface states on the bare surface 4. As noticed before, those

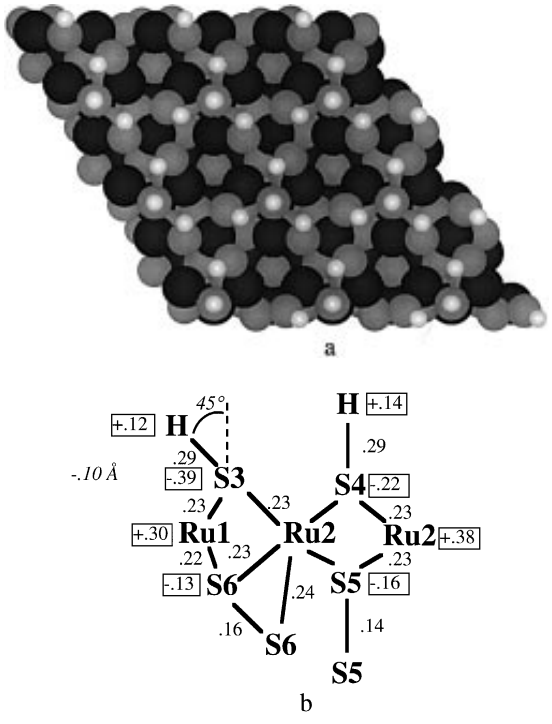

FIG. 8. A top view representation of the hydrogenated model 4 of the surface (Ru atoms are black, S atoms are gray, and H atoms are white) and a schematic describing some structural elements, the atomic charges (in a box), and overlap populations (z values for S_3 refers to the bulk).

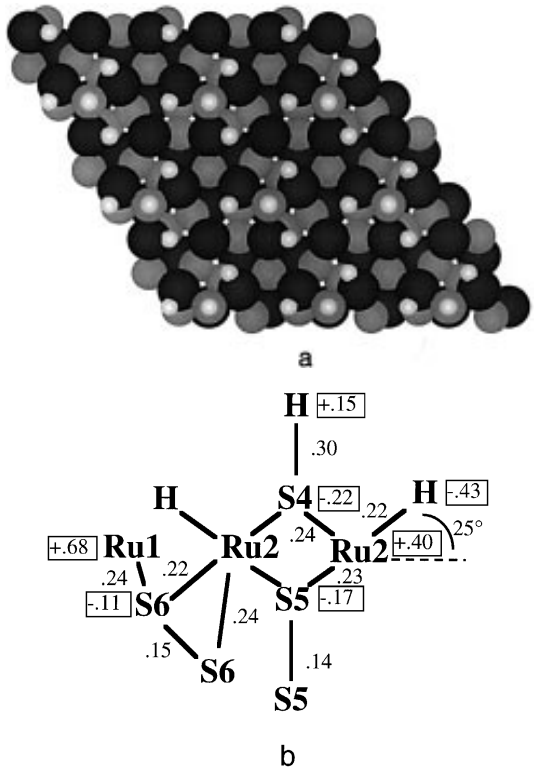

FIG. 9. A top view representation of the hydrogenated model 1 of the surface (Ru atoms are black, S atoms are gray, and H atoms are white) and a schematic describing some structural elements, the atomic charges (in a box), and overlap populations.

S-localized surface states are cancelled after adsorption (Fig. 7b).

The situation is completely different if S_3 is removed in order to consider the reduced surface 1. Ru atoms are now accessible and Ru–H bonds can be formed, together with S–H bonds. Different H coverages with 4, 5, 7, or 8 H atoms in the unit cell have been calculated. The case with 1 S–H and 3 Ru–H shown in Fig. 9 corresponds to the best chemisorption energy per H_2 molecule (−102 kcal · mol^{-1}) and also to the most stable hydrogenated surface 1 (increasing the coverage would destabilize the system compared to gas phase H_2). The optimized Ru–H distance is 1.6 Å, in good agreement with the distances obtained in metal complexes with hydrides. The two H on the surface are clearly different (Fig. 9b), the one linked to S having a small positive charge (+0.15), while that bonded to Ru has a marked hydride character with a negative charge (−0.43). The electronic structure of the slab contrasts with that of the sulfur-rich systems. There is a high-lying occupied surface state centered on the Ru atoms, which disappears after chemisorption and the top of the large (Ru–S) band has a marked metal character (Fig. 7c). Both effects are important for the possible formation of hydride. This hydrogen atom has a strong contribution on high-lying occupied states, an indication of a good reactivity, while the proton-like hydrogen

appears on more stable levels, at the bottom of the band (Fig. 7d).

V. CONCLUSION: REDUCTION OF $RuS_2(111)$ BY MOLECULAR HYDROGEN

From the comparison between the energy of those hydrogenated surfaces, it is possible to build a model for the reduction of the (111) surface of RuS_2 (Fig. 10). The starting point is the sulfur rich surface 7. All the energies here are related unless specified to the unit cell of the surface, and the origin is the bare surface 7 with 8 molecules of H_2 in the gas phase. The first H_2 molecules (two per surface unit cell) are used to hydrogenate the surface in order to get the structure of Fig. 6. S atom removal from the surface can be obtained by going to the hydrogenated surface 4 (Fig. 8) and making three H_2S molecules from the three removed S atoms, using three additional H_2 molecules. We only considered here the thermodynamic balance of the transformation and did not calculate the eventual energy barrier for the reaction. While the first hydrogenation step is strongly exothermic (-200 kcal $\cdot$ mol^{-1}, 2 H_2 molecules reacting), this first model reduction step is significantly endothermic ($+66$ kcal $\cdot$ mol^{-1} or $+22$ kcal per mole of S removed). The number of H atoms at the surface is not modified. The elimination of sulfur is difficult but would be even more so in the absence of hydrogen (it requires 279 kcal $\cdot$ mol^{-1} to go from surface 7 to surface 4, making three isolated S atoms, and 168 kcal $\cdot$ mol^{-1} if 3/2 S_2 are made instead). Two factors make the transformation easier with hydrogen: the extracted S atoms are more stabilized in H_2S than they are in S_2, and also the chemisorption energy of H_2 on surface 4 is larger (by 26 kcal $\cdot$ mol^{-1} per surface unit cell), so that the H-terminated surface is more stable. Experimentally, the reduction is not an easy process and requires a high pressure of H_2 and a high temperature. The model reaction would be clearly favored at high temperature by the entropy difference between H_2S and H_2, and at high pressure of H_2 since H_2 is a reactant.

The second step would go from the hydrogenated surface 4 to the hydrogenated surface 1, extracting three more sulfur atoms and creating the hydride species on the surface. This step is even more endothermic (180 kcal $\cdot$ mol^{-1} or $+60$ kcal per mole of S removed). Without hydrogen, the transformation from surface 4 to surface 1 requires 351 kcal $\cdot$ mol^{-1} if three isolated atoms are created and 240 kcal $\cdot$ mol^{-1} if 3/2 S_2 are made. This second transformation, where hydride species are created, is more difficult because the dissociation of H_2 is not as exothermic on surface 1 as it is on the other surfaces (the Ru–H bond is weaker than the S–H bond). It was already underlined, however, that these strongly reduced surfaces are susceptible to be stabilized by reconstruction, which could significantly reduce the endothermicity.

Therefore, it can be deduced that the H_2 molecules have various influences in the reduction process: they saturate and stabilize the RuS_2 surfaces, they facilitate the S abstraction by formation of H_2S, and they form the reactive hydride species. The calculations therefore allow to obtain a *qualitative* microscopic picture of the surface during this reduction process.

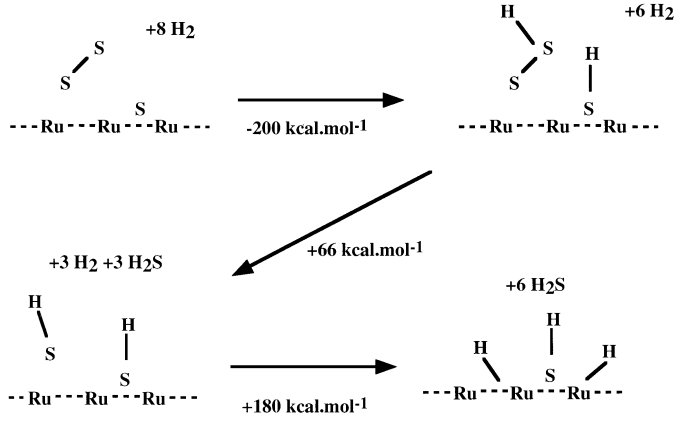

FIG. 10. A model for the reduction of the (111) surface of RuS_2 by molecular hydrogen. The starting point is the most stable model 7 (Fig. 2) with 3 tilted S_2 pairs (only one shown) and one hollow S adatom and with one H_2 gas phase molecules for each surface unit cell. The transformation goes through the hydrogenated models 7, 4, and 1 previously described, with successive formation of H_2S molecules. The enthalpy changes per surface unit cell are indicated.

ACKNOWLEDGMENTS

We thank M. Lacroix, C. Geantet, and M. Breysse for helpful discussion.

REFERENCES

1. Lacroix, M., Boutarfa, N., Guillard, C., Vrinat, M., and Breysse, M., *J. Catal.* **120**, 473 (1989).
2. Lacroix, M., Marrakchi, H., Calais, C., Breysse, M., and Forquy, C., "Heterogenous Catalysis and Fine Chemicals II" (M. Guisnet *et al.*, Eds.), p. 277. Elsevier, Amsterdam, 1991.
3. Zonnevylle, M. G., Hoffmann, R., and Harris, S., *Surf. Sci.* **199**, 320 (1988).
4. Rodriguez, J., *Surf. Sci.* **278**, 326 (1992).
5. Ruette, F., Valencia, N., and Sanchez-Delgado, R. J., *J. Am. Chem. Soc.* **111**, 40 (1989).
6. Gainza, A. E., Rodriguez-Arias, E. N., and Ruette, F., *J. Mol. Catal.* **85**, 345 (1993).
7. Anderson, A. B., Al-Saigh, Z. Y., and Hall, W. K., *J. Phys. Chem.* **92**, 803 (1988).
8. Anderson, A. B., *J. Catal.* **119**, 135 (1989).
9. Yu, J., Anderson, A. B., and Yu, J., *Mol. Catal.* **62**, 223 (1990).
10. Anderson, A.-B., and Yu, J., *J. Catal.* **119**, 135 (1989).
11. Lacroix, M., Mirodatos, C., Breysse, M., Decamp, T., and Yuan, S., *in* "Proceedings, 10th International Congress on Catalysis, Budapest, 1992," (L. Guczi, F., Solymosi, and P. Tetenyi, Eds.), p. 597. Akadémiai Kiadó, Budapest, 1993.
12. Lacroix, M., Yuan, S., Breysse, M., Dorémieux-Morin, C., and Fraissard, J., *J. Catal.* **138**, 409 (1992).

13. Jobic, H., Clugnet, G., Lacroix, M., Yuan, S., Mirodatos, C., and Breysse, M., *J. Am. Chem. Soc.* **115**, 3654 (1993).
14. Frechard, F., and Sautet, P., *Surf. Sci.*, accepted.
15. Weimer, M., Kramar, J., Bai, C., and Baldeschwieler, J. D., *Phys. Rev. B* **37**, 4292 (1985).
16. Qin, X. R., Yang, D., Frindt, R. F., and Irwin, J. C., *Phys. Rev. B* **44**, 3490 (1991).
17. Frechard, F., and Sautet, P., *Surf. Sci.* **336**, 149 (1995).
18. Dovesi, R., Saunders, and V. R., Roetti, C., CRYSTAL92, User's manual, University of Turin, Italy, and SERC Daresbury Laboratory, UK; Dovesi, R., Pisani, C., Roetti, C., and Saunders, V. R., "CRYSTAL88 in Quantum Chemistry Exchange," Indiana University, Department of Chemistry, Bloomington, IN, 1988.
19. Pisani, C., Dovesi, R., and Roetti, C., "Hartree-Fock ab initio Treatment of Crystalline Systems," Lecture Notes in Chemistry, Vol. 48. Springer-Verlag, Heidelberg, 1988.
20. Perdew, J. P., *in* "Electronic Structure of Solids" (P. Ziesche and H. Eschrig, Eds.), Akademie Verlag, Berlin, 1991.
21. Orlando, R., Dovesi, R., Roetti, C., and Saunders, V. R., *J. Phys.: Condens. Matter.* **2**, 7769 (1990).
22. Dovesi, R., Roetti, C., Freyria-Fava, C., Apra, E., Saunders, V. R., and Harrison, N. M., *Phil. Trans. R. Soc. Lond. A* **341**, 203 (1992).
23. Pacios, L. F., and Christiansen, P. A., *J. Chem. Phys.* **82**, 2664 (1985).
24. LaJohn, L. A., Christiansen, P. A., Ross, R. B., Atashroo, T., and Erlmer, W. C., *J. Chem. Phys.* **87**, 2812 (1987).
25. Shustorovitch, E., *Adv. Catal.* **37**, 101 (1990).